Open Journal of Metal, 2013, 3, 34-44
http://dx.doi.org/10.4236/ojmetal.2013.33006 Published Online September 2013 (http://www.scirp.org/journal/ojmeta)

Synthesis of Solid Acid Catalysts Based on TiO_2 - SO_4^{2-} and Pt/TiO_2 - SO_4^{2-} Applied in *n*-Hexane Isomerization

Juan Manuel Hernández Enríquez[1*], Luz Aracely Cortez Lajas[1], Ricardo García Alamilla[1], Estefanía Ángeles San Martín[1], Pedro García Alamilla[2], Edward Brent Handy[3], Guadalupe Cárdenas Galindo[3], Luz Arcelia García Serrano[4]

[1]Instituto Tecnológico de Cd. Madero, División de Estudios de Posgrado e Investigación, Juventino Rosas y Jesús Urueta S/N, Col. Los Mangos, 89440 Cd. Madero, Tamaulipas, México
[2]Universidad Juárez Autónoma de Tabasco, División Académica de Ciencias Agropecuarias, Avenida Universidad S/N, Zona Cultura, Colonia Magisterial, 86040 Villahermosa Tabasco, México
[3]CIEP, Facultad de Ciencias Químicas, Universidad Autónoma de San Luis Potosí, Av. Dr. Manuel Nava #6, Zona Universitaria, 78210 San Luis Potosí, San Luis Potosí, México
[4]Instituto Politécnico Nacional, Centro Interdisciplinario de Investigaciones y Estudios sobre Medio Ambiente y Desarrollo 30 de Junio #1520, Barrio La Laguna Ticomán, 07340 México D.F., México
Email: *jmanuelher@hotmail.com

Received June 22, 2013; revised July 22, 2013; accepted July 30, 2013

ABSTRACT

The physicochemical properties and catalytic activity of pure and sulfated titanium oxide (TiO_2 and TiO_2-SO_4^{2-}) is described in this work. Titanium hydroxide synthesized by the sol-gel method was impregnated with a 1 N H_2SO_4 solution, varying amount of sulfate ions (SO_4^{2-}) in the range from 10 to 20 wt%. Pure and modified hydroxides were calcined at 500˚C for 3 h and then characterized by TGA-DTG, XRD, BET, FT-IR, potentiometric titration with *n*-butylamine and 2-propanol dehydration. Catalytic activity of materials was tested in the *n*-hexane isomerization at 350˚C. The results showed that TiO_2 and TiO_2-SO_4^{2-} mainly developed anatase phase. All TiO_2-SO_4^{2-} have acceptable specific surface area (95 - 105 m^2/g). Potentiometric titration with *n*-butylamine revealed that TiO_2-SO_4^{2-} showed higher acidity (430 - 530 mV) than compared to pure TiO_2 (−15 mV), indicating that this oxide only has weak acidity. The results showed good relationship between acidity determined by potentiometric titration with *n*-butylamine and the catalytic activity evaluated by 2-propanol dehydration and *n*-hexane isomerization. Titanium oxide with 20 wt% of SO_4^{2-} ions was the material that demonstrated the highest catalytic activity for both reactions.

Keywords: Acid Catalysts; Sulfated Titanium Oxide; Physico-Chemical Properties; *n*-Hexane Isomerization

1. Introduction

Solid acid catalysts have assumed a great importance due to their huge application potential in chemical industry, specifically in the oil refining industry [1-4]. The super-acid liquid catalysts such as HF, H_2SO_4, $AlCl_3$ and BF_3, which are efficient and selective at low temperatures, are not profitable for such processes due to severe problems of corrosion and their difficult separation from the stream of the products. Chlorinated alumina, zeolites modified by ionic exchange, heteropolyacids, as well as some bifunctional catalysts are examples of solid acid catalysts applied in the types of processes mentioned above and also reported in the literature. Most of these catalysts suffer from various drawbacks such as high working temperature, continuous supply of chlorine and the use of high hydrogen pressure [5]. For these reasons, current researches about heterogeneous acid catalysts have been focused on the synthesis of new materials that are capable of replacing the liquid acid catalysts and halogenated solids mentioned previously. Sulfated oxide supports demonstrate strong acidity and catalytic activity at low temperatures for catalytic cracking, alkylation, and light paraffin isomerization [6-9]. One of the most studied materials for these reactions has been sulfated zirconium oxide [10-14], although the possibility of using sulfated titanium oxide (TiO_2-SO_4^{2-}) for such purposes is not discarded. The sulfate ion can be introduced from H_2SO_4, $(NH_4)_2SO_4$, SO_2 and H_2S. It was reported that the existence of covalent S-O bonds in sulfur complexes formed on metal oxides are responsible for the genera-

*Corresponding author.

tion of acidity [15-17]. The substitution of oxygen atoms in the titania lattice with sulfur and other anionic species [18] are reported to show photocatalytic activity enhancement in visible light [19,20] due to the existence of oxygen vacancies, greater surface area [21-25], and larger fraction of the anatase phase. These physicochemical properties can be controlled from the synthesis process [26]. Although most of these catalytic supports are prepared via the precipitation method [27-29], the sol-gel process offers better control over synthesis parameters, especially to obtain uniform textural and chemical characteristics down to the nanometric level [29-34]. Ohno *et al*. [35] reported the incorporation of sulfur in titania by sol-gel precipitation using titanium isopropoxide and thiourea and showed the enhancement in photocatalytic degradation of 2-propanol and partial oxidation of adamantane at wavelengths longer than 440 nm. Arata [36] synthesized sulfated titania by exposing $Ti(OH)_4$ to aqueous sulfuric acid followed by calcination. Ohno *et al*. [35] studied the hydroxylation of adamantane using sulfated titania as catalyst, a reaction of relevance (green process) using molecular oxygen. It is reported that the activity of sulfated titania could be improved by optimizing the surface area of the sample. In general, it is conceived that Brönsted and Lewis acidity are improved by modifying TiO_2 with H_2SO_4. The superacid properties of sulfated titania were considered to be responsible for the high catalytic activity in various acid-catalyzed reactions such as the alkylation of derivatives of benzene, cracking of paraffins and dimerization of ethylene [37-41]. The increase in activity for CFC-12 decomposition obtained with sulfated titania was due to the superacid properties of the catalysts [21,42]. Other reactions catalyzed by sulfated titania due to its acidic properties are acylation of aromatics [43], acylation of Friedel-Crafts [44], esterification [45] and transesterification of vegetal oils [46].

In the search for new solid acid catalysts with improved properties, this work focuses on the synthesis and characterization of a sulfated titanium oxide by sol-gel method, and presents a preliminary evaluation of its catalytic properties for the *n*-hexane isomerization reaction.

2. Experimental

2.1. Supports Preparation

The preparation of titanium hydroxide [$Ti(OH)_4$] was carried out via sol-gel by dissolving titanium *n*-butoxide IV ($Ti[O(CH_2)_3CH_3]_4$; Sigma-Aldrich; 97 wt%) in tert-butyl alcohol ($(CH_3)_3COH$; Baker; 99.6 %) and the hydrolysis and condensation proceed via the drop-wise addition of a water/tert-butyl alcohol solution. The gel was then aged during 72 h and dried at 100˚C for 24 h. $Ti(OH)_4$ impregnation with acid agent was done by the incipient wetness method, using a 1 N H_2SO_4 solution and adding the necessary amount of acid reagent to obtain supports with 10, 15 and 20 wt% of SO_4^{2-} ions. Pure and modified hydroxides were dried at 100˚C during 24 h and then calcined in dynamic air atmosphere at 500˚C for 3 h. Taking the calcination temperature and the weight percentage of SO_4^{2-} ions as reference, the synthesized materials were named as follows: T0500, T10500, T15500 and T20500. The method for the preparation of the catalytic supports is illustrated in the flow diagram of **Figure 1**.

2.2. Catalyst Preparation

To test activity for the light paraffin isomerization, the catalytic supports were impregnated with platinum (Pt) by the incipient wetness method, using an ammonia solution

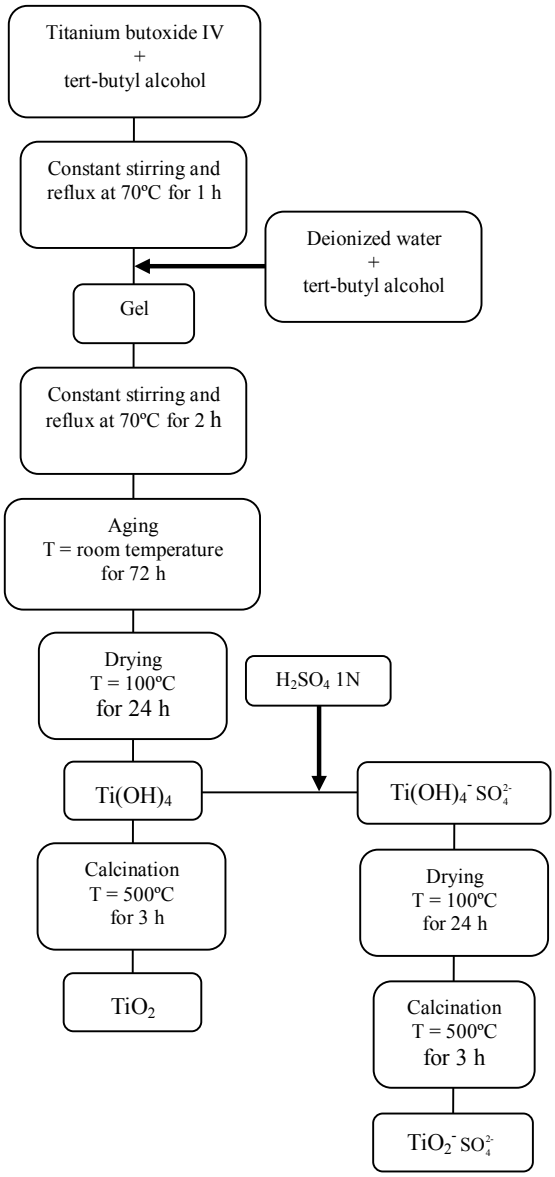

Figure 1. Flow diagram of synthesis method of titanium oxide and sulfated titanium oxide.

of $Pt(NH_3)_2(NO_2)_2$; Sigma-Aldrich; 3.4 wt%, followed by a drying at 100˚C for 6 h and a calcination in air flow at 400˚C for 3 h. The theoretical concentration of Pt was fixed at 0.3 wt% for all catalysts. The Pt-containing catalysts are designated: Pt/T0500, Pt/T10500, Pt/T15500 and Pt/T20500.

2.3. Characterization Techniques

Catalytic supports were characterized by thermal analysis, X-ray diffraction, nitrogen physisorption, infrared spectroscopy, potentiometric titration with *n*-butylamine and 2-propanol dehydration. Thermogravimetric analyses were conducted on a TA Instruments STD 2960 simultaneous DSC-TGA. The samples were analyzed in air flow (10 mL/min) at a heating rate of 10˚C/min from a room temperature to 900˚C. Powder X-ray diffraction patterns were recorded on a Bruker diffractometer using Cu Kα radiation (λ = 1.5406 Å) and a graphite secondary beam monochromator; the intensities of the diffraction lines were obtained in the 2θ range between 20 and 80˚ with a step size of 0.02˚ and a measuring time of 2.7 s per point. The crystallite size of the materials was determined with the Scherrer equation. Nitrogen physisorption was used to determine the specific surface areas of the materials at the temperature of liquid nitrogen (−196˚C) in a Quantachrome Autosorb-1 instrument. Prior to the measurements, samples were outgassed at 350˚C for 2 h. The specific surface area was calculated using the BET equation and the BJH method was used to determine the pore size distributions and the pore volume of the samples. Infrared spectroscopic analyses were carried out in a Fourier Transform spectrometer (Perkin-Elmer Spectrum One) with transparent wafers containing the sample to be analyzed and KBr as a binding agent (9:1 dilution), co-adding 16 scans at a resolution of 4 cm^{-1}. The acidity of the catalytic supports was determined by potentiometric titration with *n*-butylamine. A small quantity of *n*-butylamine dissolved in acetonitrile (0.025 M solution) was added to a known mass of solid which was suspended in the solution and stirred for 3 h. After this, the suspension was titrated with the same base at a rate of 0.2 mL/min, and the variation in the electrical potential was measured with a JENWAY-3310 digital pH meter. The potentiometric titration method used in this work has been previously reported by Cid and Pecchi [57]. In order to evaluate the acid-base properties of catalytic materials, 2-propanol dehydration reaction was performed. The reaction was carried out in a fixed-bed reactor operating at 80˚C, atmospheric pressure and WHSV = 5 h^{-1}. Approximately 0.1 g of the catalyst was loaded into the reactor. Prior to the reaction, the catalyst was preheated at 350˚C for 1 h in a purified nitrogen flow. During the reaction, the effluent collected periodically and analyzed by a Varian 3400 gas chromatograph equipped with a FID detector and a column packed with Carbowax 1540 on Chromosorb.

2.4. Catalytic Activity

The *n*-hexane isomerization was carried out in a conventional flow fixed-bed reactor, operating at 350˚C, atmospheric pressure and WHSV = 0.5 h^{-1}. The catalyst (0.3 g) was reduced at 350˚C for 1 h in a flow of hydrogen prior to running the test reaction. The products were analyzed on-line by a Varian 3400 gas chromatograph equipped with a FID detector and a column packed with 23 SP-1700 on 80/100 Chromosorb.

3. Results and Discussion

3.1. Thermal Analyses

Four different weight loss stages were identified during thermal analysis of the as-prepared titanium oxide and sulfated titanium oxide materials (**Figures 2** and **3**). The first two stages, evidenced by two DTG peaks centered at 70˚C and 160˚C correspond respectively to the elimination of water and solvent occluded in the matrix of the inorganic polymer gel. The third stage of weight loss occurs within the range of 250˚C and 400˚C and is more gradual, associated with the transformation of $Ti(OH)_4$ into TiO_2 and involves the elimination of some terminal hydroxyl groups [47,48]. The sulfated titanium oxide precursors showed a fourth weight loss stage between 400˚C and 900˚C, the DTG peaks being centered around 550˚C and attributed to the decomposition and loss of sulfate ions [49]. It should be noted that samples prepared for catalysis studies were air-calcined at 500˚C, thus sulfate levels in the catalysts may be slightly lower than the theoretical levels assumed from the incipient wetness addition of H_2SO_4. The FT-IR data (see below) clearly show the presence of sulfate groups in all three sulfated TiO_2 materials.

3.2. Textural Properties

The nitrogen physisorption results indicate that the specific surface area of the titanium oxide (35 m^2/g) increases when the sulfate ion is incorporated into the matrix of the material, yielding sulfated titanium oxides with specific surface areas in the range 95-105 m^2/g (**Table 1**). Surface area enhancement is likely due to the inhibition of titania particle sintering by the surface sulfate groups. Nitrogen adsorption-desorption isotherms and pore size distributions are shown in **Figures 4** and **5**, respectively. Pure titanium oxide (T0500) presented a type II isotherm and a very closed hysteresis loop that identifies the presence of pores with shape of cone and/or wedge [50-52]. In contrast, sulfated materials (T10500,

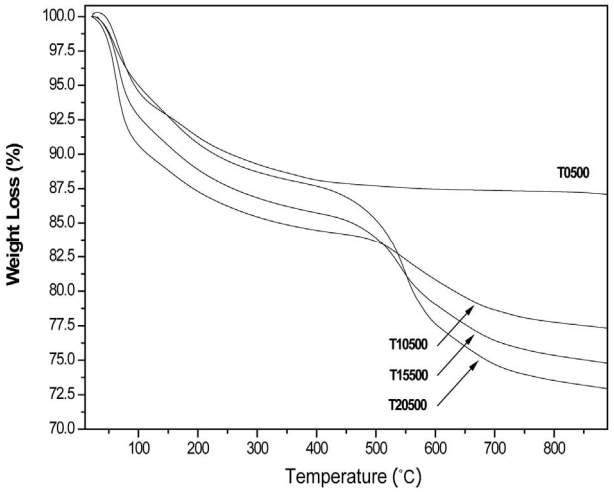

Figure 2. TG profiles developed by TiO_2 and TiO_2-SO_4^{2-} precursors.

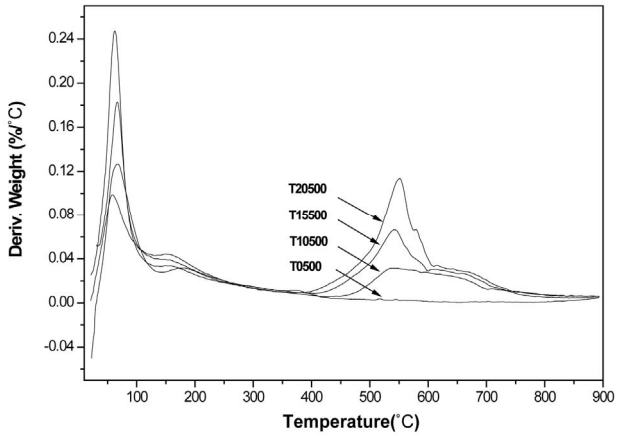

Figure 3. DTG profiles developed by TiO_2 and TiO_2-SO_4^{2-} precursors.

Table 1. Textural properties of synthesized titanium oxides.

Material	Surface area (m^2/g)	Pore diameter (Å)	Pore volume (cm^3/g)
T0500	35	673	0.05
T10500	97	28	0.13
T15500	103	34	0.14
T20500	104	49	0.16

T15500 and T20500) showed type IV isotherms with H2 hysteresis loops that represent a uniform mesoporous structure [52]. Pore size distributions were obtained by the BJH method. The sulfated titanium oxides (T10500, T15500 and T20500) presented a monomodal distribution with most frequent pore diameters in the 30 to 50 Å range. In contrast, pores in pure titanium oxide (T0500) are considerably larger (200 - 1000 Å) and the distribution is broader.

3.3. X-Ray Diffraction

Figure 6 shows the X-ray diffraction patterns obtained for pure titanium oxide (T0500) and for the sulfated titanium oxides (T10500, T15500 and T20500) calcined at 500˚C. The crystalline anatase (tetragonal) form of titania is evidenced by lines appearing at $2\theta = 25.22^\circ$, 36.97˚, 37.88˚, 38.58˚, 47.99˚, 53.90˚, 55.07˚, 62.70˚, 68.84˚ and 70.31˚, which correspond to crystallographic planes (101), (103), (004), (112), (200), (105), (211), (204), (116), and (220), in reference to JCPDS card number 021-1272. In comparison to the pure titania sample, these diffraction lines are noticeably broadened in the diffracttograms of the sulfated titania, indicative of a decrease in crystallite size [53]. Average crystal sizes were calculated using the Scherrer equation to quantify line broadening on the most intense (101) anatase peak, and results are plotted in **Figure 7** as a function of sulfate content. The average anatase crystal size decreases to one-half its value upon sulfate addition to pure titania at any of the loadings used. There is no evidence of rutile formation in any of the samples.

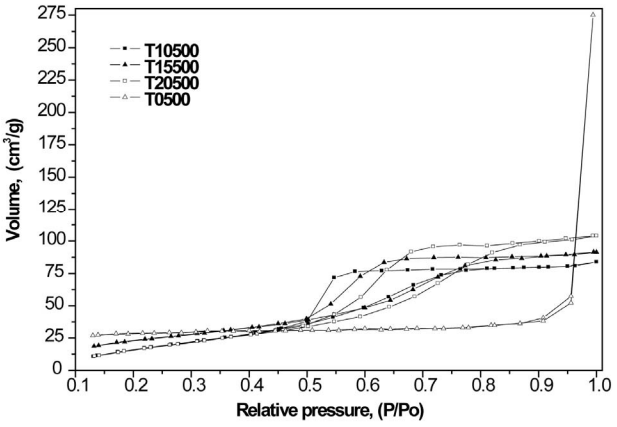

Figure 4. Nitrogen adsorption-desorption isotherms obtained with synthesized titanium oxides, TiO_2 and TiO_2-SO_4^{2-} .

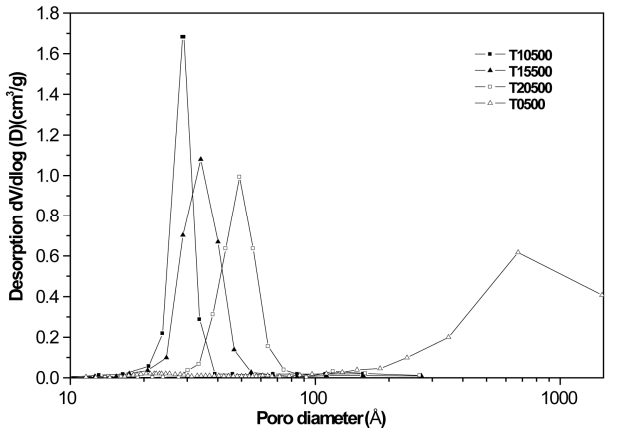

Figure 5. Pore size distribution obtained with synthesized titanium oxides, TiO_2 and TiO_2-SO_4^{2-} .

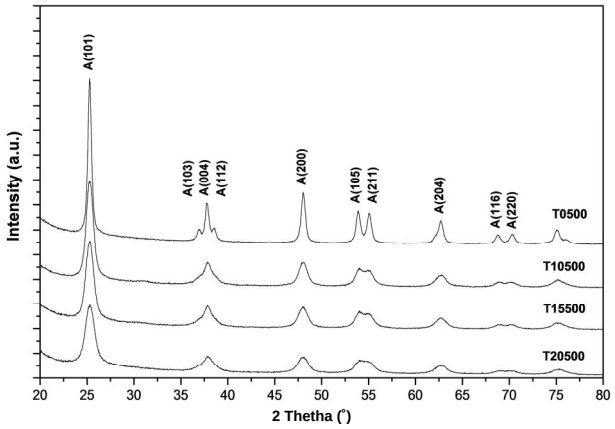

Figure 6. X-ray diffraction patterns of synthesized titanium oxides, TiO_2 and TiO_2-SO_4^{2-}.

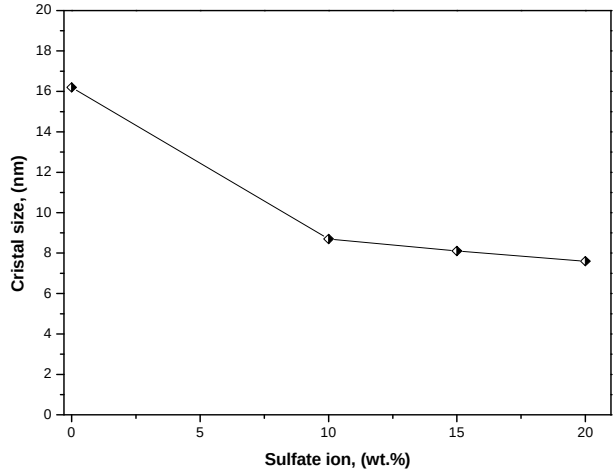

Figure 7. Crystal size as a function of sulfate ion content in the titanium oxide.

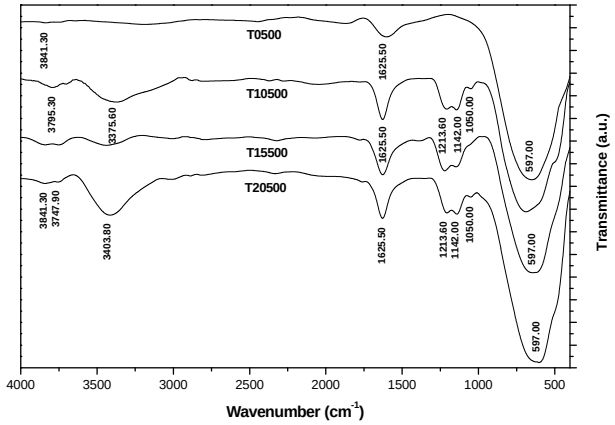

Figure 8. Infrared spectra of TiO_2 and TiO_2-SO_4^{2-}.

3.4. Infrared Spectroscopy

In **Figure 8** are shown the infrared spectroscopy analyses performed on synthesized titanium oxides. All materials of this study presented bands that appear in the 3800 - 1600 cm^{-1} region, which characterize -OH groups and hydrogen bonding. The absorption bands located at 3841, 3795, and 3747 cm^{-1} are attributed to the ν(OH) stretching vibration modes of isolated hydroxyl groups associated with Ti^{4+} cations. The broad adsorption band at 3400 cm^{-1} and the band at 1625 cm^{-1} are assigned to the stretching and bending modes characteristic of physisorbed water on oxide supports [54]. The sulfated materials (T10500, T15500 and T20500) present bands characteristic of surface SO_4^{2-} groups. In the sulfated titania samples, the bands observed at 1213, 1142, and 1050 cm^{-1} are attributed to the vibrational bands of S-O bonds in the sulfate (SO_4^{2-}) groups anchored to the titanium oxide surface [54]. The exact frequency is usually red-shifted when perturbed by the presence of physisorbed water. It is important to point out that the signals located at 3400 and 1625 cm^{-1} are intensified in the infrared spectrum of sulfated materials. From this result it can be inferred that sulfated metal oxide support materials have a greater capacity for water adsorption from moist environments than pure titanium oxide (T0500). In principle, the absence of ν(S = O) band frequency at 1370 cm^{-1} can be related to a particular degree of surface hydration, which in turn relates to the density of Brönsted and Lewis acid sites. Lewis acid sites exist at the sulfur (S^{6+}) center in the surface sulfate groups [55]. The Lewis acid site density will increase with increasing calcination temperature, as the surface progressively dehydroxylates. The broad adsorption bands that appear in the low frequency region of infrared spectrum, located in the range 450 - 600 cm^{-1} are characteristic of a Ti-O-Ti symmetric stretching vibration mode [56], which could be formed during condensation reaction of sol-gel synthesis.

3.5. Acidic Properties

The surface acidity of the synthesized titanium oxides was evaluated by potentiometric titration with *n*-butylamine. This technique makes it possible to determine the maximum acid strength (M.A.S.) through the first reading of the titration, expressed as a measure of the acidity potential (pH) or as milivolts (mV). The number of acid sites present in the synthesized materials is determined by the amount of base used [57]. The strength of acid sites can be classified according to scale reported by Pizzio *et al.* [58]: M.A.S > 100 mV (very strong acid sites), 0 < M.A.S. < 100 mV (strong acid sites), −100 < M.A.S. < 0 mV (weak acid sites), and M.A.S. < −100 mV (very weak acid sites). **Figure 9** shows how sulfate ions increase the acidity degree of the titanium oxide generating very strong acid sites on its surface, as well as a notable difference between pure titanium oxide (T0500) and the sulfated materials (T10500, T15500 and T20500). All sulfated titanium oxides showed a maximum acid

strength above 400 mV, while pure titanium oxide only reached values below zero as maximum acid strength (−15 mV). Also, the total quantity of miliequivalents of *n*-butylamine used per catalyst gram (meq *n*-BTA/g) confirmed that concentration of acid sites is greater in sulfated samples than the non-treated material (**Figure 10**).

The *n*-butylamine titration results clearly establish that sulfate groups on titania exhibit a strong acid strength, and that sulfate loading at the levels employed here (10 - 20 wt%) enables one to control the site density of these acid sites. Given the presence of hydroxyl bands in all three of the sulfated titania samples, as shown in the IR spectra, it can be inferred that the samples exhibit both Brönsted and Lewis acidity, although this was not investtigated more directly with pyridine adsorption IR studies.

3.6. 2-Propanol Dehydration

The decomposition of 2-propanol is a model reaction to determine the acid-base nature of catalytic materials and can serve as a characterization technique to evaluate the relative acidity between catalysts. It has been reported in the literature that the 2-propanol decomposition reaction can follow three possible routes: 1) intra-molecular dehydration that produce propylene, 2) inter-molecular dehydration to generate diisopropyl ether, and 3) alcohol de-hydrogenation to produce acetone [59]. It is known that, under inert atmosphere, the alcohol dehydration reactions take place through acid sites, whereas the dehydrogenation reaction is catalyzed by basic sites [60]. Thus, reaction selectivity is a measure of the relative amounts of each site type in the catalyst. The results are presented in **Table 2**. The un-sulfated titania (T0500) did not show any catalytic activity at 80˚C, whereas all three sulfated titanias were active. The activity order is the following: T20500 > T15500 > T10500, with a 4-fold activity increase going from 10 to 15 wt% sulfate, and a smaller increase when increasing sulfate content from 15 to 20 wt%. This correlates with the potentiometric titration with *n*-butylamine results showing increasing M.A.S. (**Figure 9**), although the total acid concentration does not increase in the same proportions (**Figure 10**), indicating that intrinsic site activity must change considerably, certainly when going from 10 to 15 wt% sulfate content. In **Figure 11**, the predominance of acid sites is evident, since reaction leads exclusively to the dehydration products of propylene and diisopropyl ether, the former being favored in all cases. Propylene is formed over Brönsted sites via the E1 elimination mechanism, whereas diisopropyl ether is formed via a S_N2 mechanism. The E1 mechanism, characteristic in the dehydration of secondary and tertiary alcohols, starts with the protonation of the -OH group, which then leaves as water to produce a carbenium ion. This step is unimolecular and rate-limiting, and followed by the rapid loss of a β hydrogen to the surface and desorption an olefin product. Diisopropyl ether is the lesser product, occurring via a S_N2 substitution mechanism. This occurs in a single step, (no intermediate) when one 2-propanol molecule attacks an adsorbed, protonated 2-propanol molecule prior to its forming a carbenium ion intermediate that would otherwise lead to propylene [61,62]. In this study, we attribute the formation of diisopropyl ether to the low reaction temperature used during the experiment (80˚C), which

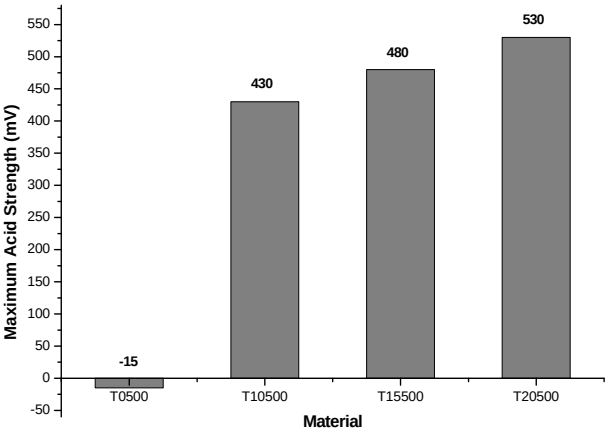

Figure 9. Maximum acid strength developed by synthesized titanium oxides (TiO_2 and TiO_2-SO_4^{2-}) determined by potentiometric titration with *n*-butylamine.

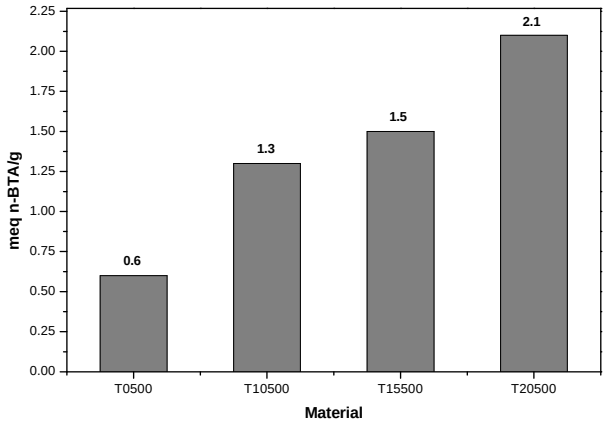

Figure 10. Total acidity obtained by potentiometric titration with *n*-butylamine for TiO_2 and TiO_2-SO_4^{2-}.

Table 2. 2-propanol dehydration, conversion and reaction rate evaluated at 60 min, T = 80˚C, P = 1 atm, WHSV = 5 h^{-1}.

Material	Conversion (%)	Reaction rate (mol g^{-1} s^{-1})
T10500	6	1.394×10^{-4}
T15500	27	6.274×10^{-4}
T20500	38	8.831×10^{-4}

limits to some extent the carbenium ion formation. The production of diisopropyl ether result is attractive, however, since this oxygenated compound can be mixed with gasoline as an additive to increase octane number.

3.7. *n*-Hexane Isomerization

The results obtained for the *n*-hexane isomerization reaction are presented in **Table 3**. The sulfated titanium oxides were active in the isomerization of hydrocarbon at 350˚C and atmospheric pressure in contrast with pure titania, which did not show catalytic activity. This fact can be explained considering that the isomerization of alkanes depends on the density of the acid sites as well as of the acid strength of the catalyst [63], parameters that are not satisfied in the non-sulfated titanium oxide, according to the results obtained by the potentiometric titration with *n*-butylamine. The materials activity obtained at 350˚C indicates that the acid strength of TiO_2-SO_4^{2-} is lower than that of ZrO_2-SO_4^{2-} because this material catalyzes the *n*-hexane isomerization at 250˚C [64]. As with the 2-propanol dehydration reaction, the catalytic activity for isomerization increases with sulfate ion content. The maximum conversion of the hydrocarbon (21%) was obtained with the catalyst Pt/T20500, a four-fold activity increase with respect to the catalyst with lowest sulfate content (Pt/T5500). All the catalysts presented excellent selectivity values around 80% for isomerized products. These selectivity values do not depend significantly of conversion level. Only monobranched paraffins such as 2-methylpentane and 3-methylpentane were identified during the reaction. The lack of 2,2-dimethylbutane formation is due to the impossibility of forming a quaternary carbon within the framework of carbenium ion chemistry and alkyl or hydride shift mechanisms [65]. The selectivity pattern suggests only minor hydrocracking activity ($<C_6$) and oligomerization activity ($>C_6$). Finally, it is clear that the catalyst with highest content of sulfate ions (Pt/T20500) presents the highest selectivity towards disintegration reactions, which require strong acid sites. This is consistent with the 2-propanol reaction and *n*-butylamine data showing that this catalyst possesses the highest total acid density and acid strength among the three sulfated samples. Hence, an effective catalyst for *n*-hexane isomerization should have a medium or low density of highly acidic sites in order to avoid side reactions and to maintain high isomerization activity.

The activity and selectivity of the Pt/T20500 catalyst was compared with that obtained by the material T20500 and both are showed in **Figure 12** and **Figure 13**, respectively. TiO_2-SO_4^{2-} has a moderate activity, although the catalytic activity rate drops very quickly and is completely lost in 120 min, while the reaction produces a lot of cracking products. We assumed that this deactivation was due to longer residence time of surface intermediates species, associated with lower hydrogen availability caused by the absence of platinum. Over Pt/ TiO_2 - SO_4^{2-}, the activity is much more stable and the selectivity for isomers are very high during the run. These results suggest that the addition of platinum and hydrogen is required to prevent the rapid deactivation of

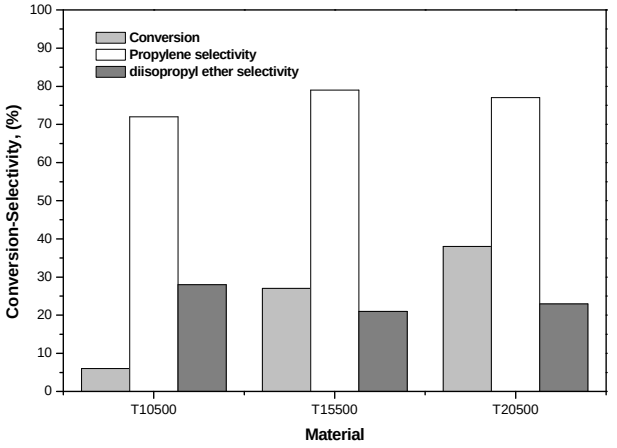

Figure 11. 2-propanol dehydration, conversion and selectivity evaluated at 60 min, T = 80˚C, P = 1 atm and WHSV = 5 h^{-1}.

Table 3. *n*-hexane isomerization with Pt/ TiO_2-SO_4^{2-} catalysts evaluated at 120 min, T = 350˚C, P = 1 atm, WHSV = 0.5 h^{-1}.

Catalyst	Conversion (%)	Selectivity (%)			
		$<C_6$	2-methylpentane	3-methylpentane	$>C_6$
Pt/T10500	5	9	45	31	15
Pt/T15500	16	6	45	32	17
Pt/T20500	21	13	44	29	14

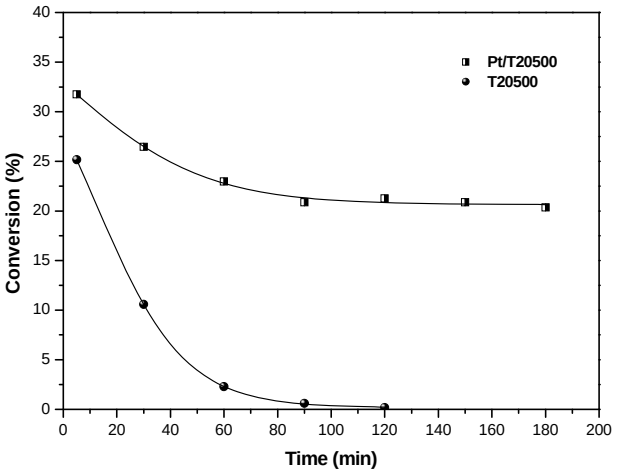

Figure 12. Conversion profiles for *n*-hexane isomerization catalyzed by TiO_2-SO_4^{2-} and Pt/ TiO_2-SO_4^{2-} catalysts. Reaction conditions: T = 350˚C, P = 1 atm, WHSV = 0.5 h^{-1}.

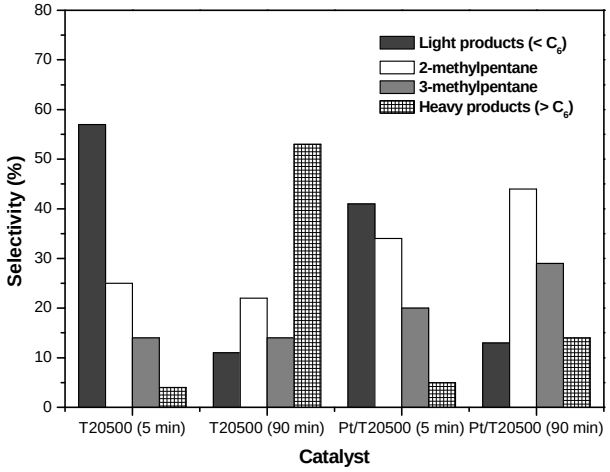

Figure 13. Selectivity to products of *n*-hexane conversion in the presence of TiO_2-SO_4^{2-} and Pt/ TiO_2-SO_4^{2-}. Reaction conditions: T = 350˚C, P = 1 atm, WHSV = 0.5 h^{-1}.

the catalyst. The role of platinum in the presence of hydrogen is still a controversial issue. Some authors report that platinum imparts a metallic catalysis function within the classical bifunctional mechanism [66]. Ebitani *et al*. [67-69] observe a promoting effect of hydrogen on the isomerization. They suggest that strong protonic acidity is generated via dissociation and spillover of hydrogen species. Iglesia *et al*. and Comelli *et al*. [70-72] also observe a promoting effect of platinum and hydrogen and attribute it to the conversion of hydrogen atoms into hydrides, accelerating the desorption of the carbenium intermediates. It is important to note that in this work, the influence of the hydrogen is always limited to low hydrogen pressures and this could lead to low conversions.

The *n*-hexane isomerization over bifunctional catalysts Pt/ TiO_2-SO_4^{2-} can be explained by the classical bifunctional mechanism including the paraffin dehydrogenation on the metal sites, the skeletal rearrangement of the olefin on the acid sites via a carbenium ion mechanism also including cracking reactions, oligomerization or cyclization and finally the rehydrogenation of the isomerized olefin on the metal sites. On the catalyst TiO_2-SO_4^{2-} the reaction can take place solely on the acid sites via a monofuncional mechanism featuring a hydride-transfer chain reaction. The sequence starts with a hydride abstraction from the hydrocarbon on the acid sites, creating the carbenium ion which is rapidly isomerized. The iso-carbenium ion is desorbed by the hydride species created in the initial step. On the catalyst TiO_2-SO_4^{2-} we speculate that the desorption step is rate-limiting, leading to an accumulation of iso-carbenium species on the surface and a fast deactivation of the material.

4. Conclusion

The addition of sulfate ions to sol-gel derived titanium hydroxide gel delays the structural transformation from the anatase to rutile phase and produces TiO_2-SO_4^{2-} supports with controlled pore structure and suitably high specific surface area (95 - 105 m^2/g) relative to the un-sulfated gel (35 m^2/g). Furthermore, the sulfated supports demonstrated strong acidity of varying site densities depending upon sulfate content up to 20 wt%. The catalytic activity for 2-propanol dehydration and *n*-hexane isomerization correlates with maximum acid strength and the total acid site densities as determined from the potentiometric titration with *n*-butylamine. The absence of acetone from 2-propanol conversion indicates that only acid sites are formed in these catalysts. The isomerization selectivity to mono-branched paraffins is favorably high and stable over the testing period for these catalysts, suggesting a viable catalytic system.

5. Acknowledgements

The authors wish to thank to División de Estudios de Posgrado e Investigación from Tecnológico de Ciudad Madero by its support given during development of this research work.

REFERENCES

[1] J. R. Shon, "Recent Advances in Solid Superacids," *Journal of Industrial and Engineering Chemistry*, Vol. 10, No. 1, 2004, pp. 1-15.

[2] K. Tanabe, M. Misono, Y. Ono and H. Hattori, "New Solids Acids and Bases," *Elsevier Science Publisher B-V*, Amsterdam, 1989, p. 300.

[3] K. Arata, "Solid Superacids," *Advances in Catalysis*, Vol. 37, 1990, pp. 165-211.

[4] B. H. Davis, R. A. Keogh and R. Srinivasan, "Sulfated Zirconia as a Hydrocarbon Conversion Catalyst," *Catalysis Today*, Vol. 20, No. 2, 1994, pp. 219-256. doi:10.1016/0920-5861(94)80004-9

[5] J. R. Shon, Y. H. Kim, B. L. Lee and H. W. Kim, "Physicochemical and Catalytic Properties of $NiSO_4$ Supported on Fe_2O_3 for Acid Catalysis," *Journal of Industrial and Engineering Chemistry*, Vol. 13, No. 6, 2007, pp. 1035-1042.

[6] X. Bokhimi, A. Morales, E. Ortiz, T. López, R. Gómez and J. Navarrete, "Sulfate Ions in Titania Polymorphs," *Journal of Sol-Gel Science and Technology*, Vol. 29, No. 1, 2004, pp. 31-40. doi:10.1023/B:JSST.0000016135.02238.0e

[7] F. Lonyi, J. Valyon, J. Engelhardt and F. Mizukami, "Characterization and Catalytic Properties of Sulfated ZrO_2-TiO_2 Mixed Oxides," *Journal of Catalysis*, Vol. 160, No. 2, 1996, pp. 279-289. doi:10.1006/jcat.1996.0146

[8] J. P. Chen and R. T. Yang, "Selective Catalytic Reduction of NO with NH_3 on SO_4^{2-} /TiO_2 Superacid Catalyst," *Journal of Catalysis*, Vol. 139, No. 1, 1993, pp. 277-288. doi:10.1006/jcat.1993.1023

[9] D. Das, H. K. Mishra, K. M. Parida and A. K. Dalai, "Preparation, Physico-Chemical Characterization and Catalytic Activity of Sulphated ZrO_2-TiO_2 Mixed Oxides," *Journal of Molecular Catalysis A*: *Chemical*, Vol. 189, No. 2, 2002, pp. 271-282. doi:10.1016/S1381-1169(02)00363-1

[10] G. D. Yadav and J. J. Nair, "Sulfated Zirconia and Its Modified Versions as Promising Catalysts for Industrial Processes," *Microporous and Mesoporous Materials*, Vol. 33, No. 1, 1999, pp. 1-48. doi:10.1016/S1387-1811(99)00147-X

[11] T. Kimura, "Development of Pt/SO_4^{2-}/ZrO_2 Catalyst for Isomerization of Light Naphtha," *Catalysis Today*, Vol. 81, No. 1, 2003, pp. 57-63. doi:10.1016/S0920-5861(03)00102-0

[12] C. R. Vera, C. L. Pieck, K. Shimizu and J. M. Parera, "Tetragonal Structure, Anionic Vacancies and Catalytic Activity of SO_4^{2-}-ZrO_2 Catalysts for *n*-Butane Isomerization," *Applied Catalysis A: General*, Vol. 230, No. 1, pp. 137-151.

[13] K. Tomishige, A. Okabe and K. Fujimoto, "Effect of Hydrogen on *n*-Butane Isomerization over Pt/SO_4^{2-}-ZrO_2 and Pt/SiO_2 + SO_4^{2-}-ZrO_2," *Applied Catalysis A*: *General*, Vol. 194-195, 2000, pp. 383-393.

[14] Y. Ono, "A Survey of the Mechanism in Catalytic Isomerization of Alkanes," *Catalysis Today*, Vol. 81, No. 1, 2003, pp. 3-16. doi:10.1016/S0920-5861(03)00097-X

[15] A. Kayo, T. Yamaguchi and K. Tanabe, "The Effect of Preparation Method on the Acidic and Catalytic Properties of Iron Oxide," *Journal of Catalysis*, Vol. 83, No. 1, 1983, pp. 99-106. doi:10.1016/0021-9517(83)90033-7

[16] T. Yamagushi, T. Jin and K. Tanabe, "Structure of Acid Sites on Sulfur-Promoted Iron Oxide," *The Journal Physical Chemistry*, Vol. 90, No. 14, 1986, pp. 3148-3152. doi:10.1021/j100405a022

[17] T. Jin, T. Yamagushi and K. Tanabe, "Mechanism of Acidity Generation on Sulfur-Promoted Metal Oxides," *The Journal Physical Chemistry*, Vol. 90, No. 20, 1986, pp. 4794-4796. doi:10.1021/j100411a017

[18] R. Asahi, T. Morikawa, T. Ohwaki, K. Aoki and Y. Taga, "Visible-Light Photocatalysis in Nitrogen-Doped Titanium Oxides," *Science*, Vol. 293, No. 5528, 2001, pp. 269-271. doi:10.1126/science.1061051

[19] A. Zaleska, P. Górska, J. W. Sobczak and J. Hupka, "Thioacetamide and Thiourea Impact on Visible Light Activity of TiO_2," *Applied Catalysis B*, Vol. 76, No. 1-2, 2007, pp. 1-8. doi:10.1016/j.apcatb.2007.05.005

[20] T. Ihara, M. Miyoshi, M. Ando, S. Sugihara and Y. Iriyama, "Preparation of a Visible-Light-Active TiO_2 Photocatalyst by RF Plasma Treatment," *Journal of Materials Science*, Vol. 36, No. 17, 2001, pp. 4201-4207. doi:10.1023/A:1017929207882

[21] D. S. Muggli and L. Ding, "Photocatalytic Performance of Sulfated TiO_2 and Degussa P-25 TiO_2 during Oxidation of Organics," *Applied Catalysis B*, Vol. 32, No. 3, 2001, pp. 181-194. doi:10.1016/S0926-3373(01)00137-0

[22] W. Y. Su, X. Z. Fu and K. M. Wei, "Effect of Sulfation on Structure and Photocatalytic Performance of TiO_2," *Acta Physico-Chimica Sinica*, Vol. 17, No. 1, 2001, pp. 28-31.

[23] X. Fu, W. A. Zeltner, Q. Yang and M. A. Anderson, "Catalytic Hydrolysis of Dichlorodifluoromethane (CFC-12) on Sol-Gel-Derived Titania Unmodified and Modified with H_2SO_4," *Journal of Catalysis*, Vol. 168, No. 2, 1997, pp. 482-490. doi:10.1006/jcat.1997.1660

[24] J. F. Tanguay, S. L. Suib and R. W. Coughlin, "Dichloromethane Photodegradation Using Titanium Catalysts," *Journal of Catalysis*, Vol. 117, No. 2, 1989, pp. 335-347. doi:10.1016/0021-9517(89)90344-8

[25] G. Colón, M. C. Hidalgo and J. A. Navío, "Photocatalytic Behaviour of Sulphated TiO_2 for Phenol Degradation," *Applied Catalysis B*: *Enviromental*, Vol. 45, No. 1, 2003, pp. 39-50. doi:10.1016/S0926-3373(03)00125-5

[26] S. N. Aisyiyah, D. S. Kusuma, A. Kristiani, J. A. Laksmono and S. Tursiloadi, "Preparation and Characterization of Sulfated Titania Catalysts for the Isomerisation of Citronellal," *International Journal of Basic & Applied Sciences*, Vol. 10, No. 6, 2010, pp. 5-10.

[27] O. Rodríguez, F. González, P. Bosh, M. Portilla and T. Viveros, "Physical Characterization of TiO_2 and Al_2O_3 Prepared by Precipitation and Sol-Gel Methods," *Catalysis Today*, Vol. 14, No. 2, 1992, pp. 243-252. doi:10.1016/0920-5861(92)80026-J

[28] E. N. S. Muccillo and D. M. Ávila, "Synthesis and Characterization of Submicron Zirconia-12 mol% Ceria Ceramics," *Ceramics International*, Vol. 25, No. 4, 1999, pp. 345-351. doi:10.1016/S0272-8842(98)00046-7

[29] S. Rossignol, F. Gerard and D. Duprez, "Effect of the Preparation Method on the Properties of Zirconia-Ceria Materials," *Journal of Materials Chemistry*, Vol. 9, No. 7, 1999, pp. 1615-1620. doi:10.1039/a900536f

[30] J. Wenzel, "Trends in Sol-Gel Processing: Toward 2004," *Journal of Non-Crystalline Solids*, Vol. 73, No. 1-3, 1985, pp. 693-699. doi:10.1016/0022-3093(85)90389-8

[31] J. D. Mackenzie, "Applications of the Sol-Gel Process," *Journal of Non-Crystalline Solids*, Vol. 100, No. 1-3, 1988, pp. 162-168. doi:10.1016/0022-3093(88)90013-0

[32] J. Livage and C. Sanchez, "Sol-Gel Chemistry," *Journal of Non-Crystalline Solids*, Vol. 145, 1992, pp. 11-19.

[33] M. Barrera, M. Viniegra, J. Escobar and J. A. De Los Reyes, "Control de las Propiedades Texturales de ZrO_2-TiO_2 Sol-Gel. Efecto de Parámetros de Síntesis," *Journal of the Mexican Chemical Society*, Vol. 46, No. 2, 2002, pp. 73-78.

[34] M. A. Santana, M. Morán, J. Hernández, S. Castillo and R. Gómez, "Physical Properties of TiO_2 Prepared by Sol-Gel under Different pH Conditions for Photocatalysis," *Superficies y Vacío*, Vol. 18, No. 1, 2005, pp. 46-49.

[35] T. Ohno, M. Akiyoshi, T. Umebayashi, K. Asai, T. Mitsui and M. Matsumura, "Preparation of S-doped TiO_2 Photocatalysis and their Photocatalytic Activities under Visible Light," *Applied Catalysis A*: *General*, Vol. 265, No. 1, 2004, pp. 115-121. doi:10.1016/j.apcata.2004.01.007

[36] K. Arata, "Preparation of Superacids by Metal Oxides for Reactions of Butanes and Pentanes," *Applied Catalysis A*: *General*, Vol. 146, No. 1, 1996, pp. 3-32.

doi:10.1016/0926-860X(96)00046-4

[37] M. Hino, S. Kobayashi and K. Arata, "Reactions of Butane and Isobutane Catalyzed by Zirconium Oxide Treated with Sulfate Ion. Solid Superacid Catalyst," *Journal of American Catalysis Society*, Vol. 101, No. 21, 1979, pp. 6439-6441. doi:10.1021/ja00515a051

[38] M. S. Scurrell, "Conversion of Methane-Ethylene Mixtures over Sulphate-Treated Zirconia Catalysts," *Applied Catalysis*, Vol. 34, 1987, pp. 109-117. doi:10.1016/S0166-9834(00)82449-5

[39] M. Hino and K. Arata, "Acylation of Toluene with Acetic and Benzoic Acids Catalyzed by a Solid Superacid in Heterogeneous System," *Journal of the Chemical Society, Chemical Communications*, Vol. 1, No. 3, 1985, pp. 112-113. doi:10.1039/c39850000112

[40] J. C. Yori, J. C. Luy and J. M. Parera, "*n*-Butane Isomerization on Solid Superacids," *Catalysis Today*, Vol. 5, No. 4, 1989, pp. 493-502. doi:10.1016/0920-5861(89)80013-6

[41] J. R. Shon and H. J. Kim, "High Catalytic Activity of NiO-TiO_2/SO_2^{2-} for Ethylene Dimerization," *Journal of Catalysis*, Vol. 101, No. 2, 1986, pp. 428-433. doi:10.1016/0021-9517(86)90270-8

[42] S. Imamura, T. Shiomi, S. Ishida, K. Utani and H. Jindai, "Decomposition of Dichlorodifluoromethane on TiO_2/SiO_2," *Industrial and Engineering Chemistry Research*, Vol. 29, No. 9, 1990, pp. 1758-1761. doi:10.1021/ie00105a003

[43] K. Tanabe, T. Yamaguchi, K. Akiyama, A. Mitoh, K. Iwabuchi and K. Isogai, "The Catalytic Synthesis of Acylated Compounds by Using Solid Superacid," 8*th International Congress on Catalysis*, Berlin, 2-6 July 1984, p. 601.

[44] W. Hua, Y. Xia, Y. Yue and Z. Gao, "Promoting Effect of Al on SO^{2-}_4/M_xO_y(M=Zr, Ti, Fe) Catalysts," *Journal of Catalysis*, Vol. 196, No. 1, 2000, pp. 104-114. doi:10.1006/jcat.2000.3032

[45] J. Lim, R. Liu and R. Zhao, "The Catalytic Synthesis of Isoamyl Butyrate by $SO_4^{2-}/TiO_2/La^{3+}$ Rare-Earth Solid Superacid," *Chinese Journal of Inorganic Chemistry*, Vol. 16, No. 5, 2000, pp. 829-832.

[46] R. M. de Almeida, L. K. Noda, N. S. Gonçalves, S. M. P. Meneghetti and M. R. Meneghetti, "Transesterification Reaction of Vegetal Oils, Using Superacid Sulfated TiO_2-Base Catalysts," *Applied Catalysis A*: *General*, Vol. 347, No. 1, 2008, pp. 100-105. doi:10.1016/j.apcata.2008.06.006

[47] Q. Sheng, S. Yuan, J. Zhang and F. Chen, "Synthesis of Mesoporous Titania with High Photocatalytic Activity by Nanocrystalline Particle Assembly," *Microporous and Mesoporous Materials*, Vol. 87, No. 3, 2006, pp. 177-184. doi:10.1016/j.micromeso.2005.06.036

[48] R. López, R. Gómez and S. Oros, "Photophysical and Photocatalytic Properties of TiO_2-Cr Sol-Gel Prepared Semiconductors," *Catalysis Today*, Vol. 166, No. 1, 2011, pp. 159-165. doi:10.1016/j.cattod.2011.01.010

[49] P. Ciambelli, D. Sannino, V. Palma and V. Vaiano, "The Effect of Sulphate Doping on Nanosized TiO_2 and MoO_x/TiO_2 Catalysts in Cyclohexane Photooxidative Dehydrogenation," *International Journal of Photoenergy*, Vol. 1, 2008, Article ID: 258631. doi:10.1155/2008/258631

[50] S. Storck, H. Bretinger and W. F. Maier, "Characterization of Micro- and Mesoporous Solids by Physisorption Methods and Pore-Size Analysis," *Applied Catalysis A*: *General*, Vol. 174, No. 1, 1998, pp. 137-146. doi:10.1016/S0926-860X(98)00164-1

[51] G. Leonfanti, M. Padovan, G. Tozzola and B. Venturelli, "Surface Area and Pore Texture of Catalysts," *Catalysis Today*, Vol. 41, No. 1-3, 1998, pp. 207-219. doi:10.1016/S0920-5861(98)00050-9

[52] K. S. W. Sing, D. H. Everett, R. A. Haul, L. Moscou, R. A. Pierotti, J. Rouquérol and T. Siemieniewska, "Reporting Physisorption Date for the Gas/Solid Systems with Special Reference to the Determination of Surface Area and Porosity," *Pure and Applied Chemistry*, Vol. 57, No. 4, 1985, pp. 603-620. doi:10.1351/pac198557040603

[53] L. González, I. Hernández, F. C. Robles, H. Dorantes and E. M. Arce, "Sonochemical Synthesis of Nanostructured Anatase and Study of the Kinetics among Phase Transformation and Coarsening as a Function of Heat Treatment Conditions," *Journal of the European Ceramic Society*, Vol. 28, No. 8, 2008, pp. 1585-1594. doi:10.1016/j.jeurceramsoc.2007.10.013

[54] D. A. Skoog and J. J. Leary, "Análisis Instrumental," Mc-Graw Hill, México City, 2003.

[55] T. Mishra, "Anion Supported TiO_2-ZrO_2 Nanomaterial Synthesized by Reverse Microemulsion Technique as an Efficient Catalyst for Solvent Free Nitration of Halobenzene," *Catalysis Communications*, Vol. 9, No. 1, 2008, pp. 21-26. doi:10.1016/j.catcom.2007.05.013

[56] J. Rubio, J. L. Oteo, M. Villegas and P. Duran, "Characterization and Sintering Behaviour of Submicrometre Titanium Dioxide Spherical Particles Obtained by Gas-Phase Hydrolysis of Titanium Tetrabutoxide," *Journal of the Chinese Chemical Society*, Vol. 32, No. 3, 1997, pp. 643-652.

[57] R. Cid and G. Pecchi, "Potentiometric Method for Determining the Number and Relative Strength of Acid Sites in Colored Catalysis," *Applied Catalysis*, Vol. 14, 1985, pp. 15-21. doi:10.1016/S0166-9834(00)84340-7

[58] L. Pizzio, P. Vázquez, C. Cáceres and M. Blanco, "Tungstophosphoric and Molybdophosphoric Acids Supported on Zirconia as Esterification Catalysts," *Catalysis Letters*, Vol. 77, No. 4, 2001, pp. 233-239. doi:10.1023/A:1013218307792

[59] Y. S. Hsu, Y. L. Wang and A. N. Ko, "Effect of the Sulfation of Zirconia on Catalytic Performance in the Dehydration of Aliphatic Alcohols," *Journal of the Chinese Chemistry Society*, Vol. 56, No. 2, 2009, pp. 314-322.

[60] J. E. Rekoske and M. A. Barteau, "Kinetics and Selectivity of 2-Propanol Conversion on Oxidized Anatase TiO_2," *Journal of Catalysis*, Vol. 165, No. 1, 1997, pp. 57-72. doi:10.1006/jcat.1997.1467

[61] R. T. Morrison and R. N. Boyd, "Química Orgánica," Pearson Educación, México City, 1998.

[62] C. G. Gómez Sierra, R. G. Márquez Nuño and F. C. Domínguez Sánchez, "Introducción a la Química Orgánica," Instituto Politécnico Nacional, México City, 2009.

[63] R. A. Comelli, C. R. Vera and J. M. Parera, "Influence of ZrO_2 Crystalline Structure and Sulfate Ion Concentration on the Catalytic Activity of SO^{2-}_4-ZrO_2," *Journal of Catalysis*, Vol. 151, No. 1, 1995, pp. 96-101. doi:10.1006/jcat.1995.1012

[64] O. B. Belskaya, I. G. Danilova, M. O. Kazakov, T. I. Gulyaeva, L. S. Kibis, A. I. Boronin, A. V. Lavrenov and V. A. Likholobov, "Investigation of Active Metal Species Formation in Pd-Promoted Sulfated Zirconia Isomerization Catalyst," *Applied Catalysis A*: *General*, Vol. 387, No. 1, 2010, pp. 5-12. doi:10.1016/j.apcata.2010.07.052

[65] J. G. Santiesteban, D. C. Calobro, C. D. Chang, J. C. Vartuli, T. J. Fiebig and R. D. Bastian, "The Role of Platinum in Hexane Isomerization over $Pt/FeO_y/WO_x/ZrO_2$," *Journal of Catalysis*, Vol. 202, No. 1, 2001, pp. 25-33. doi:10.1006/jcat.2001.3229

[66] J. C. Duchet, D. Guillaume, A. Monnier, C. Dujardin, J. P. Gilson, J. van Gestel, G. Szabo and P. Nascimento, "Isomerization of *n*-Hexane over Sulfated Zirconia: Influence of Hydrogen and Platinum," *Journal of Catalysis*, Vol. 198, No. 2, 2001, pp. 328-337. doi:10.1006/jcat.2000.3152

[67] K. Ebitani, H. Hattori and K. Tanabe, "Generation of Protonic Acid Sites Originating from Molecular Hydrogen on the Surface of Zirconium Oxide Promoted by Sulfate Ion and Platinum," *Langmuir*, Vol. 6, No. 12, 1990, pp. 1743-1744. doi:10.1021/la00102a006

[68] K. Ebitani, J. Konishi and H. Hattori, "Skeletal Isomerization of Hydrocarbons over Zirconium Oxide Promoted by Platinum and Sulfate Ion," *Journal of Catalysis*, Vol. 130, No. 1, 1991, pp. 257-267. doi:10.1016/0021-9517(91)90108-G

[69] K. Ebitani, J. Tsuji, H. Hattori and H. Kita, "Dynamic Modification of Surface Acid Properties with Hydrogen Molecule for Zirconium Oxide Promoted by Platinum and Sulfate Ions," *Journal of Catalysis*, Vol. 135, No. 2, 1992, pp. 609-617. doi:10.1016/0021-9517(92)90057-O

[70] E. Iglesia, S. L. Soled and G. M. Kramer, "Isomerization of Alkanes on Sulfated Zirconia: Promotion by Pt and by Adamantly Hydride Transfer Species," *Journal of Catalysis*, Vol. 144, No. 1, 1993, pp. 238-253. doi:10.1006/jcat.1993.1327

[71] E. Iglesia, D. G. Barton, S. L. Soled, S. Miseo, J. E. Baumgartner, W. E. Gates, G. A. Fuentes and G. D. Meitzner, "Selective Isomerization of Alkanes on Supported Tungsten Oxide Acids," *Studies in Surface Science and Catalysis*, Vol. 101, 1996, pp. 533-542. doi:10.1016/S0167-2991(96)80264-3

[72] R. A. Comelli, Z. R. Finelli, S. R. Vaudagna and N. S. Figoli, "Hydroisomerization of *n*-Hexane on Pt/SO_4^2 ZrO_2: Effect of Total and Hydrogen Partial Pressure," *Catalysis Letters*, Vol. 45, No. 3-4, 1997, pp. 227-231. doi:10.1023/A:1019088217236

